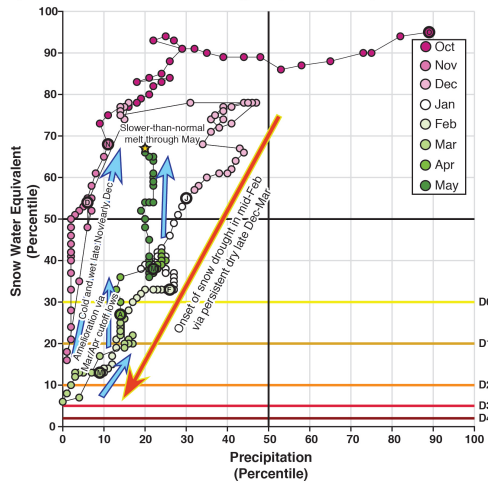

This manuscript has been submitted for possible publication in *Climate Services*. Please be aware that subsequent versions of the manuscript may be different following the formal peer-review process. If accepted for publication, the final version of this manuscript will be made available via the '*Peer-reviewed Publication DOI*' link on this page. Please do not hesitate to contact the authors to provide feedback.

Graphical Abstract

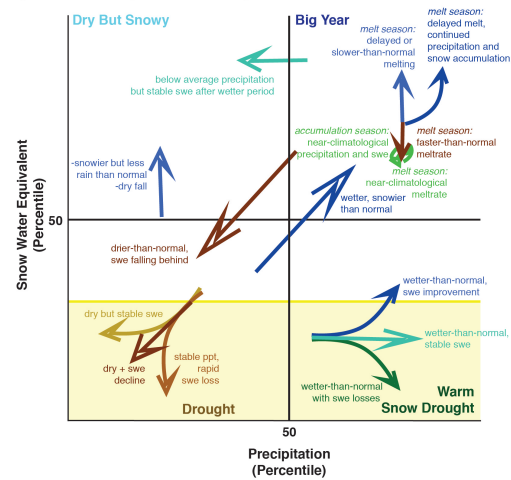
Visualizing the daily evolution and extent of snow drought

Benjamin J. Hatchett, Daniel J. McEvoy, Alan M. Rhoades

a) Central Sierra Snow Laboratory, CA (elev. 2,201 m): Water Year 2020



b) Potential Interpretations of Trajectories



Highlights

Visualizing the daily evolution and extent of snow drought

Benjamin J. Hatchett, Daniel J. McEvoy, Alan M. Rhoades

- Daily precipitation and snow water equivalent percentiles identify snow drought state
- Phase diagrams can be used to identify station, basin, and/or regional snow drought
- Snow drought timing shapes water availability, yet is often assessed at fixed times
- Gridded products can be used to reveal spatial snow drought conditions
- A web-based tool is introduced to produce real-time snow drought phase diagrams

Visualizing the daily evolution and extent of snow drought

Benjamin J. Hatchett^{a,c}, Daniel J. McEvoy^a, Alan M. Rhoades^b

^a*Western Regional Climate Center, 2215 Raggio Parkway, Reno, 89512, Nevada, USA*

^b*Climate and Ecosystem Sciences Division, Lawrence Berkeley National Laboratory, 1 Cyclotron Road, Berkeley, 94720, California, USA*

^c*Corresponding author: benjamin.hatchett@gmail.com,*

Abstract

Snow droughts are commonly defined as below average snowpack at a point in time, typically 1 April in the western United States. This definition is valuable for interpreting the state of the snowpack for resource management but obscures the temporal evolution of snow drought. Borrowing from dynamical systems theory, we applied phase diagrams to visually examine the evolution of snowpack conditions in maritime, intermountain, and continental snow climates in the western United States using station observations as well as spatially distributed estimates of snow water equivalent (SWE) and precipitation. Phase diagrams of observed SWE and precipitation percentiles highlighted snow drought onset, evolution, and termination timing at daily timescales using a percentile-based drought definition. A web tool for this visualization approach is presented that allows users to create real-time or historic phase diagrams. The goal of this tool is to facilitate the communication of snow drought conditions to broader audiences, especially in years characterized by notable hydroclimate variability and/or extreme events. Spatially distributed estimates of daily precipitation and SWE highlighted

regional and elevation-dependent variability in snow drought type and extent. When combined with additional data such as streamflow, phase diagrams and spatial estimates of snow drought conditions can inform drought monitoring and early warning as well as to help link snow drought type and evolution to observed impacts on ecosystems, water resources, and recreation.

Keywords: Drought, Hydroclimate, Monitoring, Snow, Water Resources, Visualization

1. Practical Implications

Snowpack provides essential water resources to meet ecosystem and societal demands in many regions of the world. In the western United States, seasonal mountain snowpack sustains economic well-being and provides critical ecosystem services for the region. The annual cycle of snowpack accumulation begins in fall, peaks in late winter to early spring, and melts throughout the spring to summer seasons. The total amount of water stored in the late-winter or early-spring snowpack provides a valuable indicator of warm season water availability for resource managers and whether drought conditions will improve or worsen.

Climate change is rapidly eroding the historically-assumed characteristics of the cryosphere. With the ecologic landscape and socioeconomic well-being of the western United States dependent on the mountainous hydrologic cycle, it is particularly vulnerable to sustained snowpack loss brought about by abrupt regional warming and increases in weather and climate extremes. Increased temperatures, a greater atmospheric demand for water, a higher snow-rain transition elevation, more frequent dry days, persistent drought

periods, and greater precipitation variability, including increased likelihoods of rain-on-snow and extreme winter storms, all pose challenges for managers tasked with balancing mountain precipitation, snowpack, and runoff as both a resource and a hazard.

The concept of snow drought has emerged in recent years as a useful construct to understand lower than expected snowpack, the physical origins of below average snowpack, and how its timing impacts various facets of the mountain and downstream landscapes. Snow drought is commonly defined using a point-in-time approach, typically on 1 April in the western United States when snowpacks are assumed to have reached peak water storage. In this study, we contend that this point-in-time approach obscures important diagnostics of intraseasonal snowpack variability that may better inform resource management (e.g., water supply, fire hazard, aquatic ecosystems, and recreation). A more complete perspective is needed, one that incorporates time-dependent behavior of the regional hydroclimate state and the hydrometeorological events that most shaped it. Here, we borrow from dynamical systems theory and introduce a visualization approach that allows a user to evaluate the co-variation of two key variables through time. The visualizations, called phase diagrams, report daily percentiles of accumulated water year precipitation and snow water equivalent, or the amount of meltwater stored in the snowpack. The percentile-based approach borrows from the widely-used approach of the United States Drought Monitor. Phase diagrams allow tracking of snow drought type (dry or warm), magnitude, duration, and timing over the course of the year. They also allow extreme events to be attributed as drivers of notable conditions or rapid changes in snowpack.

Importantly, they can be annotated to help more broadly communicate conditions and their evolution; thus, helping to serve and inform a larger user group that might rely on this climate information.

We provide examples of phase diagram applications across several snow-dominated regions throughout the western United States using the SNOwpack TELemetry (SNOTEL) network. The examples include the Sierra Nevada of California and Nevada (maritime), the Washington Cascades (maritime), the San Juan Mountains of Colorado (continental), and the Wasatch Mountains of Utah (intermountain). We then show how spatially distributed (or gridded) estimates of precipitation and snow water equivalent can be included in the analysis, both to highlight how spatial patterns of snowpack compare against different snow drought years and to demonstrate how watersheds can be aggregated to create basin-average snow drought phase diagrams. In the Washington example, cumulative discharge from an unimpaired stream gage is used to show the differing hydrologic outcomes of warm versus dry snow drought. Last, gridded products are used to show how the spatial extent as well as type of snow drought conditions changes throughout the course of a well-known, widespread drought year in the western United States (water year 2015).

We also share a beta version of a web-based tool, the Western Regional Climate Center’s “Snow Drought Tracker” to facilitate accessibility and communication of snow drought conditions. We use an example from the Wasatch Mountains of Utah. The Snow Drought Tracker allows users to generate phase diagram visualizations for both real-time and historic snowpack and precipitation conditions from the SNOTEL network. The default output

from the Snow Drought Tracker includes an almanac for water year 2020 conditions as well as its phase diagram. This tool, as well as the visualization concepts described herein, aim to support hydroclimate monitoring and inform drought early warning systems across the western United States. In addition to providing expert decision makers with a means to help communicate or “tell the story” of a water year to their stakeholders, we hope this tool will facilitate real-time monitoring of snow drought impacts on other aspects of the mountain environment, notably winter recreation, fire season potential and ecosystem response. The demonstrated applications of phase diagrams to gridded products indicates the phase diagram visualization concept can be transferred to regions where observational data is either non-existent or sparse.

2. Introduction

Snow-dominated mountains provide critical water resources to ecosystems and society (Viviroli et al., 2007; Sturm et al., 2017), but their snowpacks are susceptible to climate warming (Beniston, 2003; Pepin et al., 2015; Rhoades et al., 2018c). Warming impacts mountain regions in many ways, including reductions in the amount of water stored in snowpack (Mote et al., 2018), earlier springtime snowmelt (Kapnick and Hall, 2012), slower snowmelt (Muselman et al., 2017) and reductions in runoff efficiency as rain falls instead of snow (Berghuijs et al., 2014) and as atmospheric demand for moisture increases (Fisher et al., 2017). Spring snowpack is an important predictor of warm season runoff for environmental and human consumptive uses, with Livneh and Badger (2020) finding snowpack losses reduced drought prediction

skill, especially in lower elevation coastal snowpacks that are most "at risk" to warming (Nolin and Daly, 2006; Dierauer et al., 2019; Evan and Eisenman, 2021). In addition to downstream agricultural (Qin et al., 2020), environmental (Poff et al., 1997; Yarnell et al., 2020) and other economic impacts (Lund et al., 2018), snowpack reductions negatively impact wildlife (Barsugli et al., 2020) and decrease opportunities for recreation and tourism (Scott, 2006; Hatchett and Eisen, 2019; Crowley et al., 2019), which are pillars of rural mountain economies (Hagenstad et al., 2018).

Tracking snowpack throughout the western United States (western U.S.) cool season (defined broadly as October-May) and identifying below-normal snow conditions known as "snow drought" (Cooper et al., 2016; Harpold et al., 2017; Hatchett and McEvoy, 2018) aids resource managers in making informed decisions based on past, current, and forecast snowpack conditions. Often, a point-in-time approach is used by water resource management agencies to assess snowpack conditions pertaining to runoff. In fact, the date of 1 April is codified into many western U.S. water management agencies (Lynn et al., 2020) that depend on runoff from both seasonal and ephemeral snowpacks (Hatchett, 2021). The relation of this date-to-peak snowpack timing, however, varies by location and season (Trujillo and Molotch, 2014; Margulis et al., 2019). Hatchett and McEvoy (2018) highlight other challenges of the point-in-time definition. Notably, they discussed that pre-1 April snow droughts can be obscured by later heavy snowfall and that anomalous melt events during warmer-than-normal conditions can create snow drought conditions not directly related to precipitation.

These challenges, and the need to communicate mountain hydroclimate

conditions broad user groups (e.g., managers and other responsible decision makers (Marshall et al., 2020)), illustrate the need for visualization approaches that capture the signals of interest and allows tracking them through time. Here, we introduced the application of phase diagrams, which are a straightforward way to show how two variables change through time with respect to one another, to show the temporal co-evolution of snow water equivalent (SWE) and precipitation at daily timescales. We demonstrated this approach using examples from a range of western U.S. snow-dominated regions. We highlighted intraseasonal and interannual snowpack variability, snow drought variation along an elevational and longitudinal transect, and how dry snow droughts (below-average precipitation and snowpack) versus warm snow droughts (above-average precipitation but below-average snowpack) differ. A web-based tool to create phase diagrams "on the fly" is introduced: <https://wrcc.dri.edu/my/climate/snow-drought-tracker>. We also demonstrated the application of a near-real time spatial snow drought map to highlight variability in snow drought conditions across the western U.S. and within small watersheds.

3. Data

3.1. Observational Data

Daily observations of SWE and accumulated water year precipitation (the water year begins on 1 October and ends on 30 September) were acquired from seven SNOWpack TELEmetry (SNOTEL) stations from the Natural Resources Conservation Survey (<https://www.wcc.nrcs.usda.gov/snow/>) across the western U.S. (Figure 1; 1). SNOTEL is a long-term, quality-

controlled, surface-based network for observing precipitation and snow in western U.S. mountains (Serreze et al., 1999). We used SNOTEL stations located in California, Colorado, Nevada, and Washington. These stations were selected because they exemplify a diverse range of snow climates (maritime, intermountain, and continental). We acquired SNOTEL data spanning the period of record observations (typically beginning in the 1980s) for complete water years through 31 May, 2020. In our example highlighting the web-based tool, we used an end date of 8 March, 2021 to show the real-time application of phase diagrams.

Station Name	Elev. (m)	Lat ($^{\circ}$ N)	Lon ($^{\circ}$ W)	Start Date	Snow Climate
CSS Lab, CA	2201	39.33	-120.37	Oct 1983	Maritime
Mill-D North, UT	2733	40.66	-111.64	Oct 1988	Intermountain
Mount Rose Ski Area, NV	2683	39.32	-119.89	Oct 1980	Intermountain
Paradise, WA	1564	46.78	-121.75	Oct 1980	Maritime
Red Mountain Pass, CO	3414	37.89	-107.71	Oct 1980	Continental
Tahoe City Cross, CA	2072	39.32	-120.15	Oct 1980	Maritime
Virginia Lakes, CA	2866	38.07	-119.23	Oct 1978	Intermountain

Table 1: Metadata for western U.S. SNOwpack TELemetry (SNOTEL) stations used to generate the phase diagrams.

3.2. Gridded Observational Products

To add a spatial component to station-based SWE and precipitation phase diagrams, we utilized daily gridded 4 km resolution estimates of SWE for the continental U.S., herein called the University of Arizona, SWE reanalysis (UAswe; Zeng et al. (2018); Broxton et al. (2019)). The UAswe product spans water years 1982–2020. Daily gridded 4 km spatial resolution precipitation was acquired from gridMET (Abatzoglou, 2013) to provide an independent

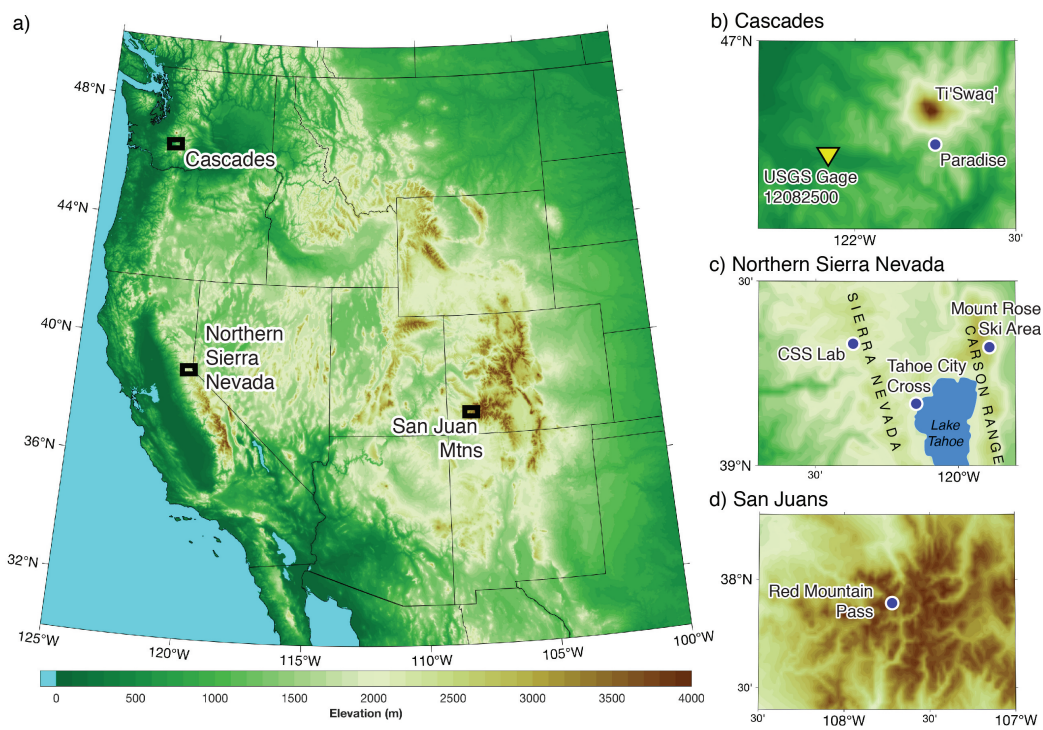


Figure 1: (A) Digital elevation map of western U.S. topography from ETOPO (Amante and Eakins, 2009) showing study areas of focus: (B) the Cascade Mountains, (C) the Northern Sierra Nevada, and (D) the San Juan Mountains. SNOTEL stations are shown by blue dots. The yellow triangle indicates the U.S. Geological Survey Gage 12082500 on the Nisqually River.

precipitation estimate from the input data (parameter-elevation regressions on independent slopes model (PRISM); (Daly et al., 2008)) to the UAswe product. Phase diagrams can be applied to any long-term daily *in-situ* and/or gridded SWE product. An example of watershed-averaged phase diagrams are presented and compared with nearby SNOTEL stations for two eight digit U.S. Geological Survey Hydrologic Unit Codes (HUC-8) watersheds (Seaber et al. (1987) in the Sierra Nevada (The Upper Yuba River Basin and the

Tuolumne River Basin). Last, we acquired daily streamflow for water years 1943–2019 from the U.S. Geological Survey Gage 12082500, located on the unimpaired Nisqually River, near the Paradise, Washington SNOTEL (1B) to show how phase diagrams can be connected to hydrologic outcomes.

4. Visualizing snow drought with a phase diagram

The concept of phase diagrams initially was developed by Ludwig Boltzmann, Henri Poincaré, and Josiah Willard Gibbs with the intent to represent all possible states of a dynamical system, such as a particle’s position and momentum (Nolte, 2010). Many disciplines use phase diagrams (also referred to as phase space diagrams)—including nonlinear dynamics, chaos theory, as well as statistical and quantum mechanics. Each parameter of the system of study is represented by an axis of a multidimensional space. In a two-dimensional system, each point on the phase plane (phase diagram) represents a combination of the system’s parameters, with the evolution of the system’s state through time tracing a line called the phase space trajectory. The phase space trajectory begins at the point representing the initial conditions. Depending on the application, the trajectory continues indefinitely or until the time period of interest has elapsed.

Inspired by the simplicity of phase diagrams, specifically the Wheeler-Hendon phase diagrams used to track the phase and life cycle of the tropical intraseasonal Madden-Julian Oscillation (Wheeler and Hendon, 2004), our purpose is to show how this visualization approach can track SWE and precipitation conditions during the cool season. We aim to track the phase space of cool season mountain hydroclimate in order to link the trajectory of snow

drought conditions (dry and warm; (Harpold et al., 2017)) to the hydrometeorological events (Hatchett and McEvoy, 2018) shaping the trajectories. Thus, phase diagrams can be used to diagnose snow drought onset, termination, duration, type, and magnitude (severity) as well as explore timing and characteristics of 'drought-busting storms'. By implicitly including these mixture effects, phase diagrams provide a unique perspective over more standard time series plots. For instance, phase diagrams can more clearly show the abrupt changes in one or both variables during notable accumulation or melt events.

4.1. Creating the snow drought phase diagram

For each station, we calculated daily percentiles of accumulated precipitation and SWE from 1 October to 31 May using a seven-day moving window centered on each calendar day. We calculated percentiles using the period of record. Following (Huning and AghaKouchak, 2020b), we used the U.S. Drought Monitor "D scale" (Svoboda et al., 2002) to characterize snow drought as abnormally dry (D0), moderate drought (D1), severe drought (D2), extreme drought (D3), and exceptional drought (D4) for values between the 30th-20th, 20th-10th, 10th-5th, 5th-2nd, and below the 2nd percentiles, respectively. Snow drought is defined as SWE percentiles less than the 30th percentile, which is slightly more inclusive than (Marshall et al., 2019), who selected the 25th percentile as their threshold but consistent with the Drought Monitor. The 80% of average threshold selected by (Hatchett and McEvoy, 2018) is likely too inclusive to be meaningful (Hatchett, 2021) and also difficult to define in places with less interannual variability. Accumulated precipitation percentiles were plotted on the abscissa and SWE percentile on the ordinate. Each daily point was coloured by the corresponding month and connected by a line to

create the phase trajectory. Snow drought severity, following the D scale, were denoted by colored lines. We defined the start of snow drought phase diagrams at the beginning of the water year (1 October). Each trajectory point is binned by a unique color for a given water year month and the first day of each month is indicated by an emboldened letter. We selected the 31 May for the termination of trajectories, denoted by a gold star.

4.2. Analysis of gridded products

For each 4 km SWE grid cell, we calculated daily percentiles of median SWE from 1 October–31 May for water years 1982–2020, again using a seven-day moving window. The same approach was performed for gridMET precipitation. Snow drought is defined similarly as above, when SWE is below the 30th percentile. HUC-8 boundaries were used to calculate basin averages for the gridded products whose grid points fell on or within the HUC-8 boundary.

4.3. Cumulative discharge calculations

Cumulative discharge at the Nisqually River U.S. Geological Survey stream gage was calculated for all complete water years starting on the first day of the water year. For each day until the end of the water year, the cumulative discharge was calculated. For each water year, we then calculated the date when 50% of the water year total cumulative discharge occurred. Median dates of 50% of water year total discharge were calculated using the full period of record.

5. Results and Discussion

5.1. An example annotated phase diagram

Water year (WY) 2020 was characterized by notable snowpack and precipitation variability throughout the cool season in the northern Sierra Nevada (Figure 2A). Both fall and late winter featured near record-low precipitation and snowpack at the Central Sierra Snow Laboratory (CSS Lab). The upper right quadrant represents wet and snowy “Big Year” conditions when both accumulated precipitation and SWE exceed the 50th percentile. The upper left indicates SWE was above median but accumulated precipitation is below median. Trajectories into this “Dry But Snowy” quadrant can result from dry fall conditions followed by appreciable snowfall, especially in places that normally receive fall precipitation as rain, or in lower elevation, warmer locations when anomalous snowfall has occurred instead of mixed rain and snow events. A drying fall is one signal of climatic change in California (Luković et al., 2021) and may induce a leftwards shift in future phase diagram trajectories during the 21st century. During the melt season, persistent cold and dry conditions can drive trajectories upwards into the first or second quadrants as snow melts slower than is expected historically, as occurred during May 2020.

Dry snow drought conditions, or meteorological drought, are identified in the lower left (third quadrant) when SWE falls into the D0-D4 range (i.e., less than 30th percentile) and accumulated precipitation is below the median. We defined warm snow drought when SWE is below the 30th percentile and accumulated precipitation is greater than the median (lower right, or fourth quadrant). To facilitate connecting various trajectories of phase diagrams with driving processes, the annotated figure is paired with a conceptual diagram

showing potential physical interpretations of trajectories (Figure 2B).

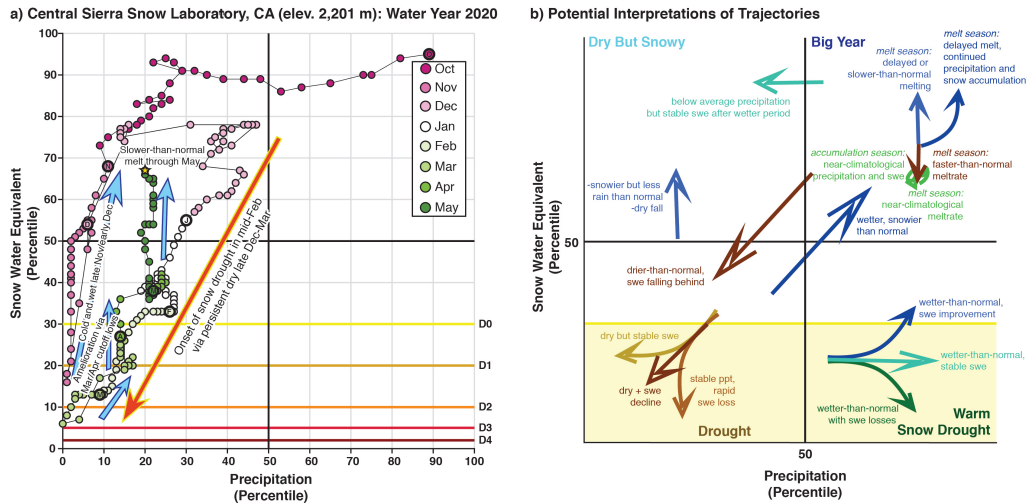


Figure 2: (A) Annotated phase diagram showing 1 October, 2019 to 31 May, 2020 at the Central Sierra Snow Laboratory (CSS Lab), California. Percentiles are calculated based on period of record data. (B) Conceptual phase diagram showing potential physical interpretations of seasonal evolution of various trajectories.

The start of WY2020 was characterized by bottom 3rd percentile precipitation conditions with low (bottom 20th percentile) snowpack at the CSS Lab (Figure 2A). Heavy precipitation falling as snow led to rapid improvement from snow drought into the “Dry But Snowy” quadrant during late November into December, with precipitation recovering to near-normal by mid-December. Persistent meteorological drought lasting from late December through mid-March, driven by a blocking ridge west of North America (Gibson et al., 2020), produced snow drought onset in late January. Above-normal temperatures, dry conditions, and seasonally induced shifts in solar insolation in late February and early March caused snowpack declines to accelerate,

reaching a minimum value in the 5th percentile. California receives the majority of its annual precipitation between December and March, meaning dry spells will quickly lead to declines in precipitation percentile (trajectories move leftward; (Figure 2A). WY2020, like other Sierra Nevada drought years, was notable for its lack of atmospheric river landfalls (Hatchett et al., 2016) that produce abrupt upwards and/or rightwards trajectories via heavy precipitation (Guan et al., 2010). Snow drought amelioration in late March occurred when heavy snowfall resulted from a slow-moving cutoff low pressure system (O’Hara et al., 2009). By 1 April, the historically assumed peak timing of snowpack in the western U.S. (e.g., Huning and AghaKouchak (2020a)), snow drought conditions remained but had improved from the 5th to nearly the 30th percentile, though precipitation remained in the bottom 15th percentile. Another cutoff low in early April provided additional snow that terminated snow drought conditions, however accumulated precipitation remained below the median. This further highlights the importance late spring (i.e., post-1 April) meteorological events in dramatically improving hydroclimatic conditions. The remainder of April and May were drier-than-normal, but snowmelt occurred slower than climatology, with above-median snowpack observed in mid-May. By annotating the phase diagram, the story of the cool season can be expressed to show the key events that produced impactful outcomes.

5.2. Snow drought variation in time and space

Weather events drive elevation-dependent changes in snowpack and snow drought conditions (Hatchett and McEvoy, 2018). In regions located near climatological expected rain-snow transition elevations (Jennings et al., 2018) such as the Sierra Nevada, individual storms can produce dramatically different

responses in snowpack spatial variability and magnitude. Atmospheric rivers are a common type of storm event yielding variable snowpack and hydrologic responses as a result of heavy precipitation with high snow line elevations (Hatchett et al., 2017; Henn et al., 2020) or with snow line elevations that vary widely over the duration of the storm (Lundquist et al., 2008; Hatchett et al., 2020).

WY2018 was emblematic of the aforementioned variation in rain and snow transition elevations as both elevation- and spatially-dependent responses to storms and dry spells occurred in the Sierra Nevada (Figure 3). By November (October omitted for clarity), WY2018 began with varying precipitation and SWE percentiles between three stations, again in the "Dry But Snowy" quadrant at the lower elevation stations (CSS Lab and Tahoe City Cross) and near climatology for the high elevation station (Mount Rose Ski Area). A late November atmospheric river event was followed by a multi-month dry spell that terminated in late February. Snowpack and precipitation conditions improved markedly in March, or what is colloquially termed a "Miracle March", due to persistent stormy conditions associated with multiple landfalling atmospheric rivers and/or midlatitude cyclones.

To highlight the heterogeneity of snowpack response within WY2018, we now investigate three different stations situated along a similar longitude. The late November warm and wet storm caused the CSS Lab and Tahoe City Cross (Figure 3A-B; both maritime snow climates) to shift rightwards and then downwards into the warm snow drought quadrant because much of the precipitation fell as rain. The CSS Lab is located along the Sierra Nevada crest while Tahoe City Cross is located further east in the rain

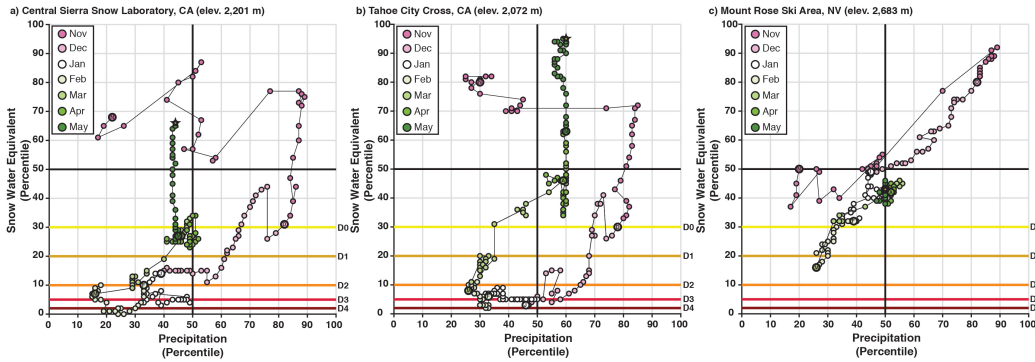


Figure 3: An elevation-longitudinal examination of snow drought conditions during water year (WY) 2018 in the northern Sierra Nevada of California and Nevada. Stations are ordered from west to east: **(A)** CSS Lab, **(B)** Tahoe City Cross, and **(C)** Mount Rose Ski Area.

shadow of the Sierra Nevada crest. The higher elevation Mount Rose Ski Area (hereafter “Mount Rose”), located further east in the Carson Range in a more intermountain snow climate (colder and drier than a maritime snow climate), received all snow. Mount Rose began the meteorological winter with 80th percentile precipitation and SWE (“Big Year”; Figure 3C). The CSS Lab and Tahoe City Cross received some snow early in December, briefly moving each location out of warm snow drought. During the subsequent dry spell, the lower elevation CSS Lab and Tahoe City Cross stations both moved leftward from warm snow drought into dry snow drought, with a 30 percentile point decline in SWE through December. Dry snow drought conditions began at Mount Rose in early February. Importantly, the role of elevation is highlighted (~600 meter range between stations) with the colder Mount Rose experiencing less dramatic snowpack declines (reaching a minimum of the 16th percentile) compared to the warmer CSS Lab (minimum of 1st percentile) and Tahoe

City Cross (minimum of 2nd percentile).

The return of an active North Pacific storm track during late February into March (or a “Miracle March”) brought notable improvement in precipitation and snowpack conditions. This month also highlighted the role of snow climate and elevation in snow drought amelioration. During this period, Mount Rose received all precipitation as snow. As a result, SWE improved by 30 percentile points (out of snow drought) while precipitation improved from the 26th percentile to 52nd percentile (Figure 3C). The maritime CSS Lab (Figure 3) improved SWE by 35 percentile points from the lowest on record for the date in late February to non-snow drought conditions by late March. Precipitation also improved by approximately 35 percentile points, back to near median values. The cold March storms demonstrated a weaker rain shadow and generally low, cold snow levels. This favored improvements in SWE at Tahoe City Cross from the 2nd percentile to above the 40th percentile while precipitation also improved from the 26th to the 60th percentile between late February and early April (Figure 3B). As a result of this “Miracle March”, 1st of April SWE conditions were closer to median than reflected by the majority of the winter, similar to WY2020 (Figure 2A). Notably, if one were to only use 1 April to identify snow drought conditions to infer potential water year reservoir recharge and/or allocations, no stations satisfied snow drought constraints, despite all stations undergoing various snow drought conditions throughout the cold-season. Importantly, the record to near-record low, late winter SWE at the lower elevation CSS Lab and Tahoe City Cross are hidden by a single point-in-time perspective. WY2018 as well as WY2020 further demonstrates the importance of a complete water year perspective,

namely the importance of a few large precipitation events in ameliorating snow drought conditions.

5.3. Warm versus dry snow drought and implications for runoff timing

The warming-induced shift in precipitation phase from snow to rain is a historic trend in the western U.S. (Lynn et al., 2020) that is projected to continue in a warmer world (Klos et al., 2014; Rhoades et al., 2018c). Precipitation phase transition from snow to rain will result in more frequent warm snow droughts (Marshall et al., 2019; Huning and AghaKouchak, 2020b). This increase will disproportionately impact climatologically warmer maritime snow climates (Dierauer et al., 2019) as well as alter the hydrology and reservoir management strategies of these watersheds (Huang et al., 2018; Rhoades et al., 2018a; Yan et al., 2018; Rhoades et al., 2018b; Ullrich et al., 2018).

The WY2015 warm snow drought in the Pacific Northwest was a motivating and formative WY for the development of snow drought research (Cooper et al., 2016). To provide a comparison of years with similar SWE anomalies, that also satisfy snow drought constraints, but different precipitation and hydrologic outcomes, we compared a dry snow drought (WY2001; Figure 4A) to the WY2015 warm snow drought (Figure 4B) at Paradise, Washington in the Pacific Northwest on the south flank of Ti'Swaq' (Mount Rainier; Figure 1B). Paradise spent the majority of the cool season of WY2001 in the bottom 10th precipitation percentile, a substantial difference from WY2015 when precipitation was between the 60th and 88th between December and April. The warm snow drought resulted from an anomalous amount of precipitation largely falling as rain in the early portion of winter. Snowpack conditions marginally improved throughout WY2001 from below the 10th

percentile in February to the 20th percentile by the end of the cool season (Figure 1A). However in WY2015, Paradise maintained fairly consistent SWE percentiles below the 10th percentile from February to May. The leftward trajectory of precipitation during February 2015 is indicative of drier-than-normal conditions followed by generally dry conditions (Figure 1B). While weak snow drought amelioration occurred in 2001, none occurred in 2015.

Figure 4 shows the entire WY phase diagrams (A-B) and snapshot in time SWE spatial extents (D-K), relative to median climatology, for WY2001 and WY2015. We also highlight the differences in hydrologic outcomes between these dry and warm snow drought years (Figure 4C). WY2001 had the second lowest cumulative flows for the Nisqually River in the period studied (WY1943–2019), but 50% of the cumulative WY2001 flow occurred 30 days *later* than the median date (3rd of April) at which half the Nisqually flow occurs. In contrast, WY2015 demonstrated middle-of-the-range total WY flow (48th of 77 years) but achieved 50% of the water year flow 56 days *earlier* than average. This indicates a large volume of water was not stored as snow for later release into the river. Depending on reservoir conditions and operations rules across varying watersheds in the Cascades, this water may not have been allowed to be captured and stored for later use. During both seasons, despite the vastly different precipitation regimes, spatial SWE anomalies are not markedly different during mid-December (Figures 4D and 4H), mid-January (Figures 4E and 4I), or late February (Figures 4F and 4J). Consistent with lower SWE percentiles at Paradise during WY 2015 compared to WY 2001 as shown on the phase diagrams, SWE anomalies are modestly more negative. The lack of mountain snowpack during WY 2015

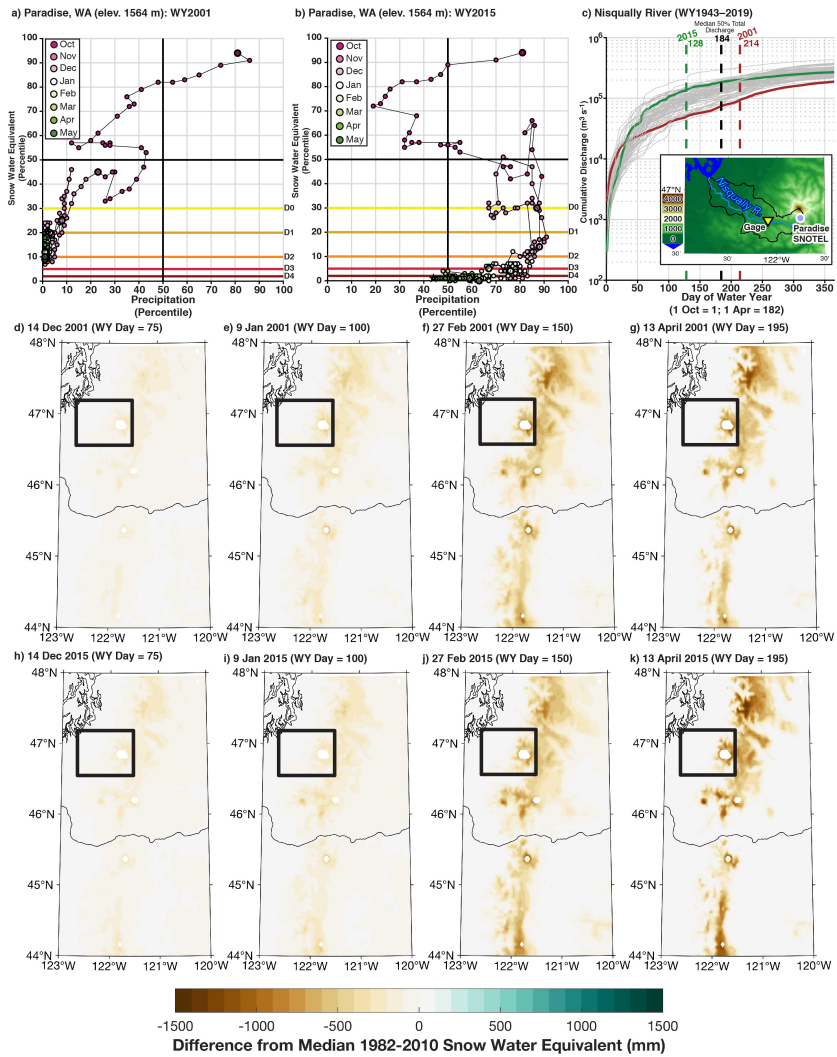


Figure 4: Comparison of dry (A) and warm (B) snow drought conditions in the Pacific Northwest at Paradise, Washington during water years (WY) 2001 and 2015, respectively. (C) Cumulative discharge from the Nisqually River with vertical dashed lines indicating the date at which 50% of the total WY runoff occurred. (D–G) Spatial snow water equivalent anomalies during WY2001 from the UAswe product (Zeng et al., 2018). (H–K) As in (D–G) but for WY2015.

was more notable than WY 2001 (Figures 3G and 4K). The comparatively better spring snowpack in WY2001 likely helped maintain streamflow later into the year despite an otherwise dry year.

5.4. *Interannual Variability*

Phase diagrams allow direct comparisons of years for case studies of interannual variability within a given region. Enhanced interannual hydroclimate variability is another robust projection of a warming climate (Boer, 2009; Pendergrass et al., 2017) with comparisons of extreme years and their outcomes providing valuable object lessons for water managers and other resource planners (Hossain et al., 2015; Sterle et al., 2019). Red Mountain Pass, located in a high elevation, continental snow climate within the San Juan Mountains of southwestern Colorado, is used to compare two late cool season outcomes that represent two hydroclimatic extremes. The majority of WY2011 showed phase trajectories in the ‘Big Year’ first quadrant (Figure 5A) after a slightly below-average start to snowpack totals between October and early December. An active December increased SWE and precipitation percentiles. Active weather continued in April and May, preventing snowmelt and causing precipitation and SWE percentiles to increase. WY2012 began with above-average precipitation and snowpack in fall but drier-than-normal conditions throughout winter which resulted in dry snow drought onset in December (Figure 5B). Modest snow drought amelioration occurred in early March, but with a few exceptions in April, dry conditions persisted through May. This led to the re-onset of dry snow drought via rapid snowmelt and below-normal precipitation.

Spatial SWE distributions (Figure 5C-J) are consistent with the phase

diagrams. In both years, SWE anomalies increased throughout the accumulation season and then accelerated in late spring. Compared to the emerging drought signal during WY2012, WY2011 did not demonstrate widespread positive SWE anomalies throughout the year. Between January and April, lower elevation regions experienced below-normal SWE anomalies (Figure 5C-D), whereas higher elevations had above-normal SWE. This difference resulted from above-normal temperatures and below-normal precipitation, with snow-albedo feedbacks (Groisman et al., 1994; Stieglitz et al., 2003) likely enhancing low elevation melting.

5.5. Basin-averaged snow drought phase diagrams

Aggregating spatially distributed information to the HUC-8 scale allows the creation of phase diagrams where no *in situ* observations exist. If such observations do exist, watershed-aggregated phase diagrams can be compared against station data, as shown in Figure 6 for water year 2020 (see Section 5.1). We examine two Sierra Nevada watersheds, the relatively low elevation Upper Yuba River Basin and the relatively high elevation Tuolumne River Basin. Both have nearby SNOTEL stations, the CSS Lab station sits at the headwaters of the Yuba River while the Virginia Lakes station is located on the lee of the Sierra Nevada crest downstream from the Tuolumne River Basin.

In both cases, similarities exist between the SNOTEL and watershed-aggregated phase diagrams. The SNOTEL stations, which are located at higher elevation than much of each watershed, show wetter (above median) and snowier (above median) early season conditions during October and November (Figure 6A,C) whereas the watersheds show below median SWE

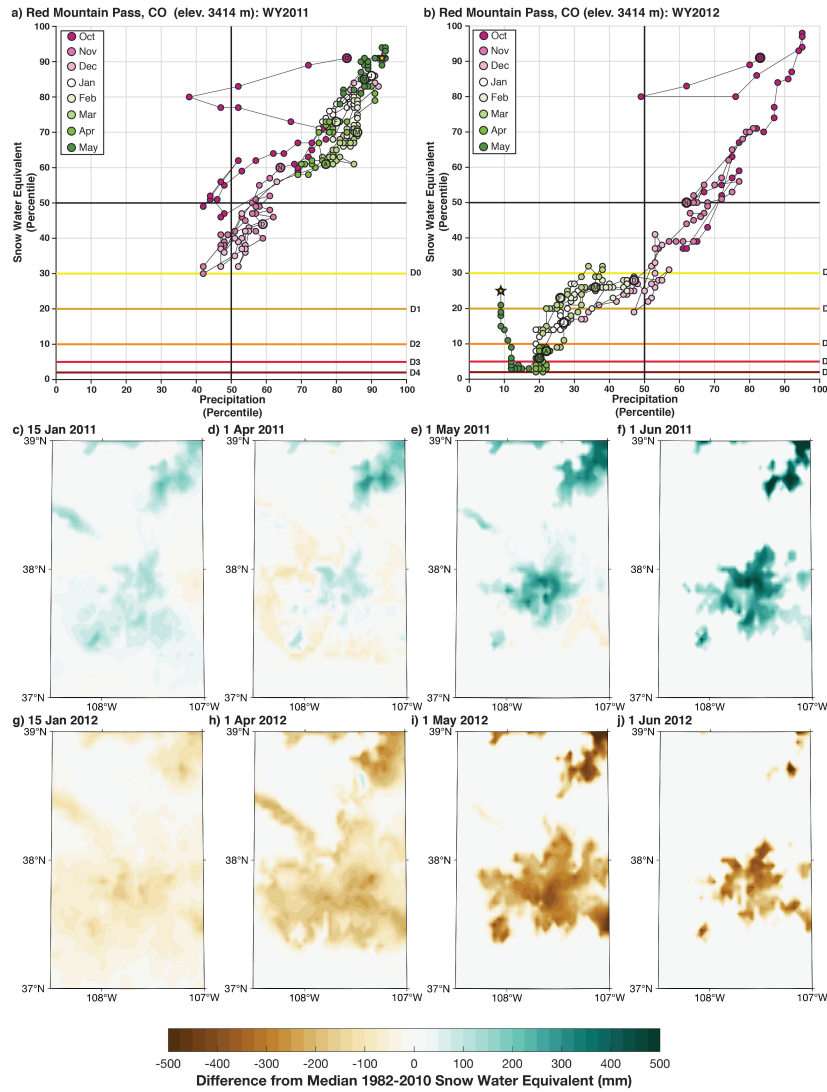


Figure 5: Comparison of an anomalously snowy and wet “big year” (A) and anomalously dry year (B) in the San Juan Mountains at Red Mountain, Colorado during water years (WY) 2011 and 2012, respectively. (C-F) Spatial snow water equivalent anomalies during WY2011 for midwinter, early, middle, and late spring from the UAswe product (Zeng et al., 2018). (G-J) As in (C-F) but for WY2012.

and precipitation (Figure 6B,D). As previously noted, late November and December brought substantial SWE improvement, with the Upper Yuba Basin moving into the "Dry But Snowy" quadrant (Figure 6B) and the Tuolumne River Basin extending further rightwards into the "Big Year" quadrant (Figure 6D). Virginia Lakes also improved into the "Dry But Snowy" quadrant (Figure 6C). Both regions followed similar trajectories downwards and to the left (SWE and precipitation falling behind; (Figure 2B) during the extremely dry period spanning late December into mid-March and then underwent modest SWE recoveries with the active spring (Miracle March).

By the end of the cool season (1 May), the higher elevation Tuolumne River Basin experienced wetter conditions (22nd percentile) compared to the Upper Yuba Basin (5th percentile precipitation) as well as exiting D0 snow drought (SWE > 30th percentile precipitation) while the Upper Yuba Basin remained in D2 (22th percentile SWE). This may reflect orographically enhanced precipitation and/or higher snowline elevation during the spring storms. The SNOTEL stations, likely by virtue of their location at higher elevation, demonstrate opposite melt-out signals to the basin-aggregated phase diagrams. The SNOTELs increased in SWE percentile through May while the basins decline. This result may stem from the inclusion of lower elevation terrain in the basin aggregations whose snow rapidly melts out during drought years (accelerated by snow-albedo feedbacks). The basin-aggregated phase diagrams appear reasonably representative in capturing the broader hydroclimate conditions interpreted from phase trajectories. Additional comparisons in other snow climates across more years are being performed; these comparisons also include independent station observations

(i.e., not used in producing the gridded SWE product) for comparison.

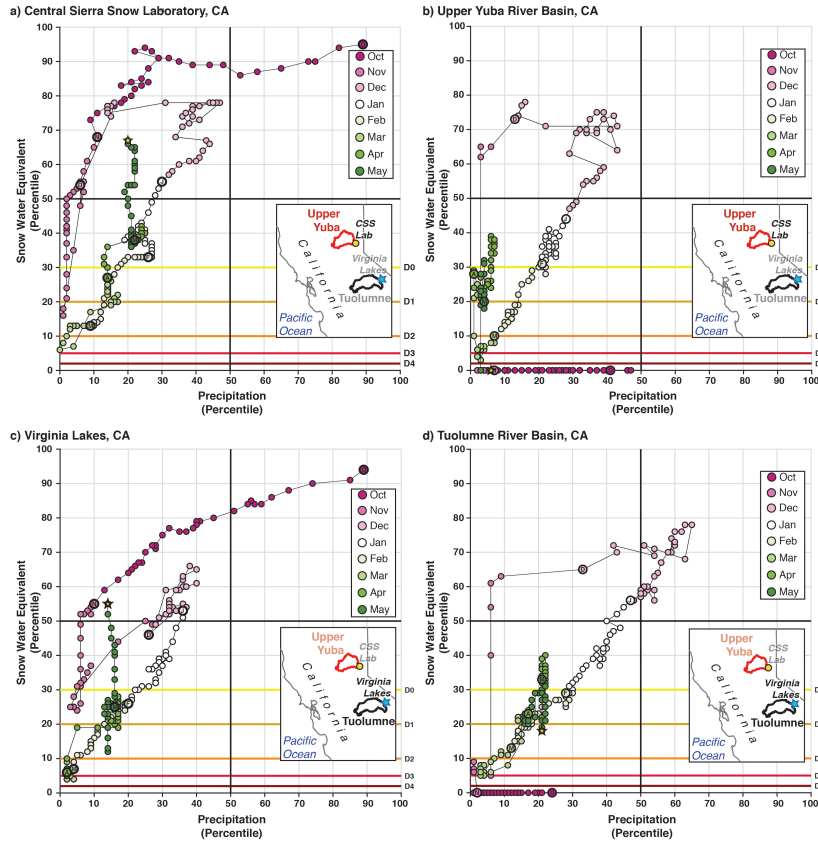


Figure 6: Phase diagrams for water year 2020: (A) CSS Lab SNOTEL, (B) Upper Yuba River Basin HUC-8, (C) Virginia Lakes SNOTEL, and (D) Tuolumne River Basin HUC-8. Locations of watersheds and SNOTEL stations are noted on inset maps.

6. Phase Diagram Limitations

Our snow drought phase diagram visualization approach is not without limitations. By failing to include additional environmental controls on snow-pack, such as temperature, radiation, and relative humidity, phase diagrams

cannot tell a complete story of the drivers of snow accumulation, ablation, and/or melt. For example, the signal of a rain-on-snow event (McCabe et al., 2007) was captured in the snow drought phase diagrams for Tahoe City Cross (see Figure 3) for an anomalously warm April atmospheric river (Hatchett, 2018) that resulted in precipitation percentiles increasing but SWE percentiles remaining constant. However, when a rain-on-snow event increases net SWE, the phase diagram will not explicitly differentiate this from a snow accumulation event. Dry periods have differing snowpack outcomes during both the accumulation and ablation season depending on temperature (Hatchett and McEvoy, 2018; Xu et al., 2019) as well as how the snowpack energy budget is influenced by spring dust deposition on snow (Skiles and Painter, 2016), cloud cover (Sumargo and Cayan, 2018), and moisture (Harpold and Brooks, 2018). How best to include these additional parameters that help to describes changes in the phase diagram trajectories will be an area of future research. Collaborations with natural resource managers and other practitioners and decision makers will be instrumental in the development of locally- or regionally-specific snow drought thresholds. Ideally, such collaborations will facilitate phase diagrams becoming part of sub-seasonal-to-inter-annual WY monitoring efforts and be used to evaluate past hydroclimatic extremes in order to evaluate approaches that may improve water supply options in a changing climate (Sterle et al., 2019).

7. Towards visualizing the type and extent of snow drought across space

We applied station data to create the phase diagrams, but a challenge in mountain environments is the lack of reliable, well-distributed, long-term observations. In lieu of station data, gridded observational products commonly inform natural resource decision-making and research efforts. The necessary components exist to create phase diagrams using gridded meteorological products (Daly et al., 2008; Abatzoglou, 2013), observationally-based snow datasets (Zeng et al., 2018; Margulis et al., 2016); or output from hydrological simulations (Livneh et al., 2015). Climate projections are also often provided in gridded format. The challenge is how to aggregate spatial information to become meaningful in complex terrain, and we have performed a first step towards this goal. Initial methods to broaden the approach could be performed by: (1) binning regions by similar elevation, watershed, slope, aspect, and/or land cover type; (2) identifying areas that co-vary together in time and space using techniques such as principal component or cluster analysis; and (3) subjective grouping based on anecdotal information from managers. Creating meaningful phase diagrams using spatially distributed information is the primary goal of our ongoing research. This will allow evaluation of snow drought in regions without long-term snow-observing networks such as in the northeastern U.S. or other high mountain areas worldwide. Towards this end, we now provide examples of how spatially distributed products can be used to visualize snow drought.

Using WY2015 as an example, we show how gridded SWE and precipitation show the spatial extent and type of snow drought. Peak warm snow drought

conditions in the Pacific Northwest were occurring in January (Figure 7A), consistent with the Paradise SNOTEL phase diagram (Figure 4B). In January, much of the Intermountain West and Rocky Mountain regions had near-average or above average (percentiles greater than the 50th, represented in purple), while several ranges in the southern tier of the western U.S. (e.g., California’s Sierra Nevada, the southern Basin and Range, and the Uinta Mountains in Utah) were experiencing dry snow drought conditions. By the 1st of February (Figure 7B) an expansion of areas experiencing dry snow drought occurred throughout the central and southern Rocky Mountains. Warm snow drought had started to transition to dry snow drought in the Pacific Northwest. Dry conditions continued through February (Figure 7C). By the 1st of April, when peak water storage in seasonal snowpacks are expected, nearly all mountain regions were undergoing snow drought conditions (Figure 7D), with the exception being the far northern Rockies, a few small areas in the Colorado Rockies, and the far northern Cascades.

The transition to dry snow drought in the Pacific Northwest (Figure 7D) was also observed at Paradise (Figure 4B). While the hydrologic outcome of the early winter warm snow drought included earlier runoff timing resulting from more frequent mid-winter runoff following rain-on-snow and rain-instead of snow ((Hatchett and McEvoy, 2018); Figure 4C), the 1st of April state of the Pacific Northwest hydroclimate indicate dry snow drought both spatially (Figure 7D) and at the station level (Figure 4B). This demonstrates the value of tracking snow drought and precipitation through time, as following the temporal evolution of hydroclimate allows outcomes (e.g., runoff characteristics and snowpack anomalies across the landscape) to be better explained. Such

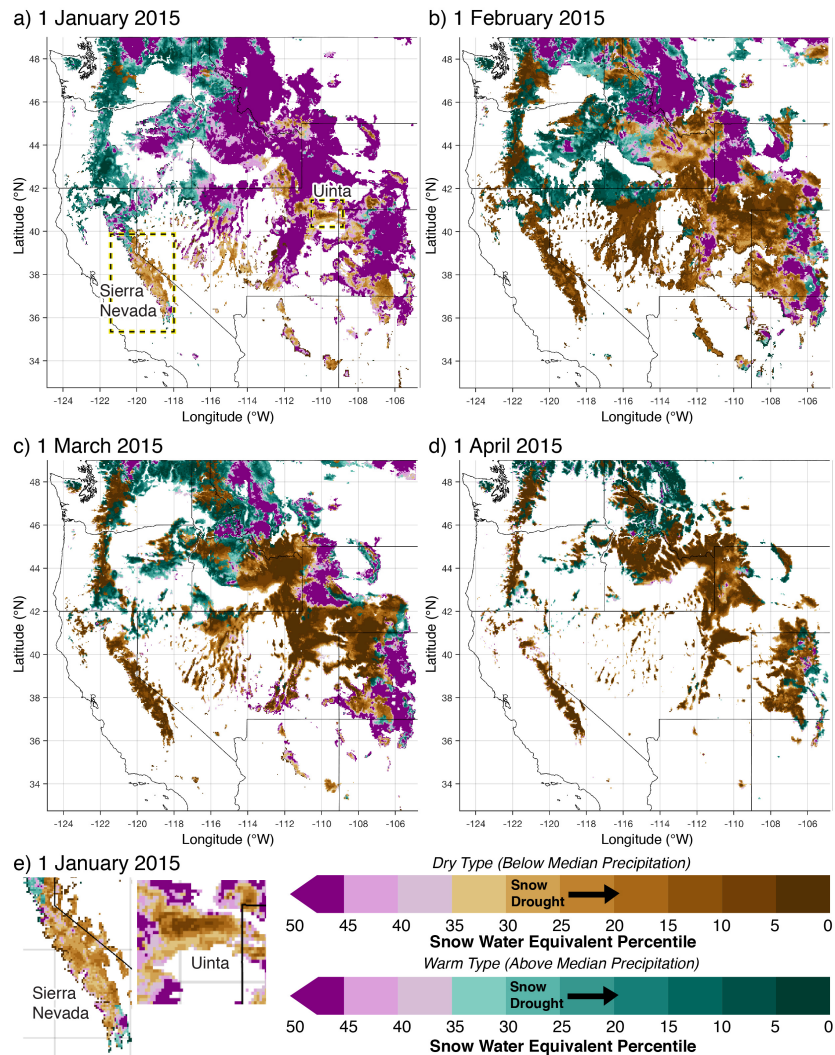


Figure 7: Spatial extent of snow drought conditions across the western U.S. on: (A) 1 January 2015, (B) 1 February 2015, (C) 1 March 2015, and (D) 1 April 2015. (E) The differing elevational patterns of snow drought in the Sierra Nevada (percentiles increase with increasing elevation) and the Uinta Mountains (percentiles decrease with increasing elevation). For clarity, only grid cells observing seasonal snowpacks (Hatchett, 2021) are shown.

explanation is important, as similar end-of-season SWE anomalies in space (compare Figures 4G, 4K, and 7D) demonstrate markedly different hydrologic outcomes (Figure 4C). Last, Figure 7E highlights an example of the differing elevational response of snow drought in the Sierra Nevada (percentiles increase with increasing elevation) and the Uinta Mountains (percentiles decrease with increasing elevation) for the same time snapshot in the WY (mid-winter) and highlights how sub-seasonal snowpack heterogeneity could influence local-to-regional water management decisions differently across the western U.S.

8. The WRCC Web-based snow drought tracker description

The snow drought tracker web application (beta version available at: <https://wrcc.dri.edu/my/climate/snow-drought-tracker>; users are required to set up a username/password to log in) was developed by the Western Regional Climate Center to provide users access to snow drought phase diagrams. These web tools are updated in near real-time across the Western United States and Alaska. The SNOTEL network (Serreze et al., 1999) is the backbone of the tool with over 700 stations that provide daily SWE, snow depth, precipitation, and temperature data. An interactive map (Figure 8A-B) allows for station selection by zooming into the region of interest. Once a station is selected, current year observations are displayed on the “Dashboard” (Figure 8C-D). As an example, the Mill-D North station in the Wasatch Mountains of northern Utah is shown. The Dashboard will also display the most recent daily updated phase diagram (starting on October 1st of the current water year; Figure 8E). The Almanac has several tabs showing

daily SWE, snow depth, and precipitation absolute values, and percent of average SWE (Figure 8C). Note that because percent of average is more commonly used by managers, the first iteration of the tool uses percent of average (and the 80% threshold) instead of percentiles and Drought Monitor thresholds as shown previously in this manuscript. From the Almanac the month-to-date, calendar year-to-date, and water year-to-date precipitation values and percent of normal can be viewed (Figure 8D). In addition to the current year data found on the dashboard, historical data and graphics can be generated. Phase diagrams can be created for any year in the station record and daily timeseries plots can be generated for SWE, snow depth, precipitation, and temperature. As an example, the daily timeseries of SWE for the period of record is generated (Figure 8E). Figures are available to download as PNG or SVG files and historical data can be downloaded in CSV format. Beta-testing of the snow drought tracker v1.0 is being conducted by stakeholders such as the National Weather Service, California Department of Water Resources, and state climatologists around the western U.S. Other agencies will be encouraged to test the tool after the first round of testing and updates have concluded. Feedback from the testing will be incorporated into future upgrades of the snow drought tracker, with the goal of further developing a web-based product that facilitates and provides a science-to-service-to-practice interface (Jacobs and Street, 2020). Some known limitations and gaps in the current version of the tool include lack of spatial snow drought information (i.e., gridded data estimates such as shown in Figure 7 or river basin composites as shown in Figure 6), the need to incorporate elevation gradients into snow drought monitoring, and the need

for longer SWE records for more robust snow drought classifications.

9. Conclusions

Our primary goal was to demonstrate a visualization approach to show the temporal evolution of snow drought conditions, and more broadly mountain hydroclimatic conditions, through the cool season. When annotated, phase diagrams help “tell the story” of a snow season and can help communicate the weather and climate events that shaped the outcome of peak snowpack and behaviour of the snowpack throughout the cool season. We provided examples showing a range of applications in various snow climates for extreme years and how additional data such as spatially distributed SWE and precipitation as well as river discharge can augment the information shown in phase diagrams. The spatial snow drought maps and basin-aggregated phase diagrams generated using gridded data products demonstrate an approach evaluating snow drought patterns across the landscape or in sparsely observed regions.

Our approach can be extended beyond addressing the noted limitations. While our primary purpose was to show the evolution of conditions in the current year, phase diagrams are easily produced for all previous years to allow comparisons of trajectories at seasonal or monthly timescales. These diagrams can be extended using forecasts of precipitation and SWE to show how snow drought conditions may evolve at subseasonal-to-seasonal timescales. For example, inclusion of bias corrected ensembles of medium range to subseasonal forecasts of precipitation and SWE from various forecasting center model(s) can create an ensemble of plausible trajectories (or cone of uncertainty) that

would provide a probabilistic perspective to explore snow-drought evolution. They can also be applied to investigate how climate change may permanently alter phase diagram trajectories and/or residence times of WY snowpack conditions in particular quadrants of the phase diagram.

Ultimately, phase diagrams may become useful tools to provide climate services to public and decision-making audiences. The goal of these diagrams and the web-based tool is to alleviate some management concerns outlined in [Hossain et al. \(2015\)](#) and [Sterle et al. \(2019\)](#), namely through illuminating water supply uncertainties and enhancing the flexibility of subseasonal-to-seasonal water management practices. Further, by providing another means to communicate climate information, phase diagrams may help further develop the capacity to identify and to rapidly evaluate underlying vulnerabilities within and between human and natural systems that are susceptible to cascading and compounding effects ([Jacobs and Street, 2020](#)). The Web-based tool that produces the snow drought phase diagrams (<https://wrcc-staging.dri.edu/my/climate/snow-drought-tracker>) presented herein is concurrently being shared with groups responsible for communicating snowpack and mountain hydroclimate information to the public such as the National Weather Service as well as water and natural resource managers and their partners. We anticipate this information will ultimately aid mountain hydroclimate monitoring and drought early warning efforts.

Conflict of Interest Statement

The authors declare that the research was conducted in the absence of any commercial or financial relationships that could be construed as a potential

conflict of interest.

Author Contributions

Benjamin J. Hatchett: Conceptualization, Investigation, Visualization, Software, Formal Analysis, Writing – Original Draft, Writing – Review and Editing, Funding Acquisition. **Daniel J. McEvoy:** Conceptualization, Investigation, Funding Acquisition, Writing – Review and Editing. **Alan M. Rhoades:** Conceptualization and Writing - Review and Editing.

Funding

Authors Hatchett and McEvoy was supported by the Desert Research Institute Foundation under an Institutional Research Project (IRP) grant and the National Weather Service Climate Services grant. Author Rhoades was funded by the Office of Biological and Environmental Research of the U.S. Department of Energy within the Regional and Global Climate Modeling Program program under the “the Calibrated and Systematic Characterization, Attribution and Detection of Extremes (CASCADE)” Science Focus Area (award no. DE-AC02-05CH11231) and the “A Framework for Improving Analysis and Modeling of Earth System and Intersectoral Dynamics at Regional Scales” project (award no. DE-SC0016605).

Acknowledgments

We appreciate feedback from Michael Anderson, Sasha Gershunov, Tim Bardsley, and Zach Tolby. Roger Kreidberg provided technical editing and writing advice.

References

- Abatzoglou, J.T., 2013. Development of gridded surface meteorological data for ecological applications and modelling. *International Journal of Climatology* 33, 121–131. doi:<https://doi.org/10.1002/joc.3413>.
- Amante, C., Eakins, B.W., 2009. ETOPO1 Global Relief Model converted to PanMap layer format. doi:[10.1594/PANGAEA.769615](https://doi.org/10.1594/PANGAEA.769615).
- Barsugli, J.J., Ray, A.J., Livneh, B., Dewes, C.F., Heldmyer, A., Rangwala, I., Guinotte, J.M., Torbit, S., 2020. Projections of mountain snowpack loss for wolverine denning elevations in the rocky mountains. *Earth's Future* 8, e2020EF001537. doi:<https://doi.org/10.1029/2020EF001537>,
- Beniston, M., 2003. Climatic change in mountain regions: A review of possible impacts. *Climatic Change* 59, 5–31. doi:[10.1023/A:1024458411589](https://doi.org/10.1023/A:1024458411589).
- Berghuijs, W.R., Woods, R.A., Hrachowitz, M., 2014. A precipitation shift from snow towards rain leads to a decrease in streamflow. *Nature Climate Change* 4, 583–586. doi:[10.1038/nclimate2246](https://doi.org/10.1038/nclimate2246).
- Boer, G.J., 2009. Changes in interannual variability and decadal potential predictability under global warming. *Journal of Climate* 22, 3098–3109. doi:[10.1175/2008JCLI2835.1](https://doi.org/10.1175/2008JCLI2835.1).
- Broxton, P., Zeng, X., Dawson, N., 2019. Daily 4 km gridded swe and snow depth from assimilated in-situ and modeled data over the conterminous us, version 1. Boulder, Colorado USA. NASA National Snow and Ice Data Center Distributed Active Archive Center. 1982–2017, Accessed April 2020. doi:<https://doi.org/10.5067/OGGPB220EX6A>.

- Cooper, M.G., Nolin, A.W., Safeeq, M., 2016. Testing the recent snow drought as an analog for climate warming sensitivity of cascades snowpacks. *Environmental Research Letters* 11, 084009. doi:[10.1088/1748-9326/11/8/084009](https://doi.org/10.1088/1748-9326/11/8/084009).
- Crowley, N., Doolittle, C., King, J., Mace, R., Seifer, J., 2019. Drought and outdoor recreation: Impacts, adaptation strategies, and information gaps in the intermountain west. *NIDIS Drought Report* , 1–89.
- Daly, C., Halbleib, M., Smith, J.I., Gibson, W.P., Doggett, M.K., Taylor, G.H., Curtis, J., Pasteris, P.P., 2008. Physiographically sensitive mapping of climatological temperature and precipitation across the conterminous united states. *International Journal of Climatology* 28, 2031–2064. doi:[10.1002/joc.1688](https://doi.org/10.1002/joc.1688).
- Dierauer, J.R., Allen, D.M., Whitfield, P.H., 2019. Snow drought risk and susceptibility in the western united states and southwestern canada. *Water Resources Research* 55, 3076–3091. doi:<https://doi.org/10.1029/2018WR023229>.
- Evan, A., Eisenman, I., 2021. A mechanism for regional variations in snowpack melt under rising temperature. *Nature Climate Change* doi:[10.1038/s41558-021-00996-w](https://doi.org/10.1038/s41558-021-00996-w).
- Fisher, J.B., Melton, F., Middleton, E., Hain, C., Anderson, M., Allen, R., McCabe, M.F., Hook, S., Baldocchi, D., Townsend, P.A., Kilic, A., Tu, K., Miralles, D.D., Perret, J., Lagouarde, J.P., Waliser, D., Purdy, A.J., French, A., Schimel, D., Famiglietti, J.S., Stephens, G., Wood, E.F.,

2017. The future of evapotranspiration: Global requirements for ecosystem functioning, carbon and climate feedbacks, agricultural management, and water resources. *Water Resources Research* 53, 2618–2626. doi:<https://doi.org/10.1002/2016WR020175>.
- Gibson, P.B., Waliser, D.E., Guan, B., DeFlorio, M.J., Ralph, F.M., Swain, D.L., 2020. Ridging associated with drought across the western and southwestern united states: Characteristics, trends, and predictability sources. *Journal of Climate* 33, 2485–2508. doi:[10.1175/JCLI-D-19-0439.1](https://doi.org/10.1175/JCLI-D-19-0439.1).
- Groisman, P.Y., Karl, T.R., Knight, R.W., 1994. Observed impact of snow cover on the heat balance and the rise of continental spring temperatures. *Science* 263, 198–200. doi:[10.1126/science.263.5144.198](https://doi.org/10.1126/science.263.5144.198).
- Guan, B., Molotch, N.P., Waliser, D.E., Fetzer, E.J., Neiman, P.J., 2010. Extreme snowfall events linked to atmospheric rivers and surface air temperature via satellite measurements. *Geophysical Research Letters* 37. doi:<https://doi.org/10.1029/2010GL044696>.
- Hagenstad, M., Burakowski, E., Hill, R., 2018. The economic contributions of winter sports in a changing climate. Technical Report .
- Harpold, A., Dettinger, M., Rajagopal, S., 2017. Defining snow drought and why it matters, *eos*, 98. EOS 98.
- Harpold, A.A., Brooks, P.D., 2018. Humidity determines snowpack ablation under a warming climate. *Proceedings of the National Academy of Sciences* 115, 1215–1220. doi:[10.1073/pnas.1716789115](https://doi.org/10.1073/pnas.1716789115).

- Hatchett, B.J., 2018. Snow level characteristics and impacts of a spring typhoon-originating atmospheric river in the Sierra Nevada, USA. *Atmosphere* 9, 233. doi:[10.3390/atmos9060233](https://doi.org/10.3390/atmos9060233).
- Hatchett, B.J., 2021. Seasonal and ephemeral snowpacks of the conterminous united states. *Hydrology* , 2020110545doi:[10.20944/preprints202011.0545.v1](https://doi.org/10.20944/preprints202011.0545.v1).
- Hatchett, B.J., Boyle, D.P., Garner, C.B., Kaplan, M.L., Putnam, A.E., Bassett, S.D., 2016. Magnitude and frequency of wet years under a megadrought climate in the western great basin, usa. *Quaternary Science Reviews* 152, 197–202. doi:<https://doi.org/10.1016/j.quascirev.2016.09.017>.
- Hatchett, B.J., Cao, Q., Dawson, P.B., Ellis, C.J., Hecht, C.W., Kawzenuk, B., Lancaster, J.T., Osborne, T.C., Wilson, A.M., Anderson, M.L., Dettinger, M.D., Kalansky, J.F., Kaplan, M.L., Lettenmaier, D.P., Oakley, N.S., Ralph, F.M., Reynolds, D.W., White, A.B., Sierks, M., Sumargo, E., 2020. Observations of an extreme atmospheric river storm with a diverse sensor network. *Earth and Space Science* 7, e2020EA001129. doi:<https://doi.org/10.1029/2020EA001129>. e2020EA001129 2020EA001129.
- Hatchett, B.J., Daudert, B., Garner, C.B., Oakley, N.S., Putnam, A.E., White, A.B., 2017. Winter snow level rise in the northern sierra nevada from 2008 to 2017. *Water* 9.
- Hatchett, B.J., Eisen, H.G., 2019. Brief communication: Early season snowpack loss and implications for oversnow vehicle recreation travel planning. *The Cryosphere* 13, 21–28. doi:[10.5194/tc-13-21-2019](https://doi.org/10.5194/tc-13-21-2019).

- Hatchett, B.J., McEvoy, D.J., 2018. Exploring the origins of snow drought in the northern sierra nevada, california. *Earth Interactions* 22, 1–13. doi:[10.1175/EI-D-17-0027.1](https://doi.org/10.1175/EI-D-17-0027.1).
- Henn, B., Musselman, K.N., Lestak, L., Ralph, F.M., Molotch, N.P., 2020. Extreme runoff generation from atmospheric river driven snowmelt during the 2017 oroville dam spillways incident. *Geophysical Research Letters* 47, e2020GL088189. doi:<https://doi.org/10.1029/2020GL088189>. e2020GL088189 2020GL088189.
- Hossain, F., Arnold, J., Beighley, E., Brown, C., Burian, S., Chen, J., Mitra, A., Niyogi, D., Pielke, Sr., R., Tidwell, V., Wegner, D., 2015. What Do Experienced Water Managers Think of Water Resources of Our Nation and Its Management Infrastructure? *PLOS ONE* 10, 1–10. doi:[10.1371/journal.pone.0142073](https://doi.org/10.1371/journal.pone.0142073).
- Huang, X., Hall, A.D., Berg, N., 2018. Anthropogenic Warming Impacts on Today's Sierra Nevada Snowpack and Flood Risk. *Geophysical Research Letters* 45, 6215–6222. doi:<https://doi.org/10.1029/2018GL077432>.
- Huning, L.S., AghaKouchak, A., 2020a. Approaching 80 years of snow water equivalent information by merging different data streams. *Scientific Data* 7, 333. doi:[10.1038/s41597-020-00649-1](https://doi.org/10.1038/s41597-020-00649-1).
- Huning, L.S., AghaKouchak, A., 2020b. Global snow drought hot spots and characteristics. *Proceedings of the National Academy of Sciences* 117, 19753–19759. doi:[10.1073/pnas.1915921117](https://doi.org/10.1073/pnas.1915921117).

- Jacobs, K.L., Street, R.B., 2020. The next generation of climate services. *Climate Services* 20, 100199.
- Jennings, K.S., Winchell, T.S., Livneh, B., Molotch, N.P., 2018. Spatial variation of the rain–snow temperature threshold across the Northern Hemisphere. *Nature Communications* 9, 1148. doi:[10.1038/s41467-018-03629-7](https://doi.org/10.1038/s41467-018-03629-7).
- Kapnick, S., Hall, A., 2012. Causes of recent changes in western north american snowpack. *Climate Dynamics* 38, 1885–1899. doi:[10.1007/s00382-011-1089-y](https://doi.org/10.1007/s00382-011-1089-y).
- Klos, P.Z., Link, T.E., Abatzoglou, J.T., 2014. Extent of the rain-snow transition zone in the western u.s. under historic and projected climate. *Geophysical Research Letters* 41, 4560–4568. doi:<https://doi.org/10.1002/2014GL060500>.
- Livneh, B., Badger, A.M., 2020. Drought less predictable under declining future snowpack. *Nature Climate Change* 10, 452–458. doi:[10.1038/s41558-020-0754-8](https://doi.org/10.1038/s41558-020-0754-8).
- Livneh, B., Bohn, T.J., Pierce, D.W., Munoz-Arriola, F., Nijssen, B., Vose, R., Cayan, D.R., Brekke, L., 2015. A spatially comprehensive, hydrometeorological data set for mexico, the u.s., and southern canada 1950–2013. *Scientific Data* 2, 150042. doi:[10.1038/sdata.2015.42](https://doi.org/10.1038/sdata.2015.42).
- Luković, J., Chiang, J.C.H., Blagojević, D., Sekulić, A., 2021. A later onset of the rainy season in california. *Geophysical Research Let-*

- ters n/a, e2020GL09350. doi:<https://doi.org/10.1029/2020GL090350>.
e2020GL09350 2020GL090350.
- Lund, J., Medellin-Azuara, J., Durand, J., Stone, K., 2018. Lessons from california's 2012-2013;2016 drought. *Journal of Water Resources Planning and Management* 144, 04018067. doi:[10.1061/\(ASCE\)WR.1943-5452.0000984](https://doi.org/10.1061/(ASCE)WR.1943-5452.0000984).
- Lundquist, J.D., Neiman, P.J., Martner, B., White, A.B., Gottas, D.J., Ralph, F.M., 2008. Rain versus snow in the sierra nevada, california: Comparing doppler profiling radar and surface observations of melting level. *Journal of Hydrometeorology* 9, 194–211.
- Lynn, E., Cuthbertson, A., He, M., Vasquez, J.P., Anderson, M., Abatzoglou, J.T., Hatchett, B.J., 2020. Technical note: Precipitation-phase partitioning at landscape scales to regional scales. *Hydrology and Earth Systems Science* Accepted. doi:<https://doi.org/10.5194/hess-24-1-2020>.
- Margulis, S.A., Cortés, G., Giroto, M., Durand, M., 2016. A Landsat-Era Sierra Nevada Snow Reanalysis (1985–2015). *Journal of Hydrometeorology* 17, 1203–1221. doi:[10.1175/JHM-D-15-0177.1](https://doi.org/10.1175/JHM-D-15-0177.1).
- Margulis, S.A., Liu, Y., Baldo, E., 2019. A joint landsat- and modis-based reanalysis approach for midlatitude montane seasonal snow characterization. *Frontiers in Earth Science* 7, 272. doi:[10.3389/feart.2019.00272](https://doi.org/10.3389/feart.2019.00272).
- Marshall, A.M., Abatzoglou, J.T., Link, T.E., Tennant, C.J., 2019. Projected changes in interannual variability of peak snowpack amount and timing

- in the western united states. *Geophysical Research Letters* 46, 8882–8892. doi:<https://doi.org/10.1029/2019GL083770>.
- Marshall, A.M., Foard, M., Cooper, C.M., Edwards, P., Hirsch, S.L., Russell, M., Link, T.E., 2020. Climate change literature and information gaps in mountainous headwaters of the Columbia River Basin. *Regional Environmental Change* 20, 134. doi:[10.1007/s10113-020-01721-7](https://doi.org/10.1007/s10113-020-01721-7).
- McCabe, G.J., Clark, M.P., Hay, L.E., 2007. Rain-on-snow events in the western united states. *Bulletin of the American Meteorological Society* 88, 319–328. doi:[10.1175/BAMS-88-3-319](https://doi.org/10.1175/BAMS-88-3-319).
- Mote, P.W., Li, S., Lettenmaier, D.P., Xiao, M., Engel, R., 2018. Dramatic declines in snowpack in the western us. *npj Climate and Atmospheric Science* 1, 2. doi:[10.1038/s41612-018-0012-1](https://doi.org/10.1038/s41612-018-0012-1).
- Musselman, K.N., Clark, M.P., Liu, C., Ikeda, K., Rasmussen, R., 2017. Slower snowmelt in a warmer world. *Nature Climate Change* 7, 214–219. doi:[10.1038/nclimate3225](https://doi.org/10.1038/nclimate3225).
- Nolin, A.W., Daly, C., 2006. Mapping “At Risk” Snow in the Pacific Northwest. *Journal of Hydrometeorology* 7, 1164–1171. doi:[10.1175/JHM543.1](https://doi.org/10.1175/JHM543.1).
- Nolte, D.D., 2010. The tangled tale of phase space. *Physics Today* 63, 33–38. doi:[10.1063/1.3397041](https://doi.org/10.1063/1.3397041).
- O’Hara, B.F., Kaplan, M.L., Underwood, S.J., 2009. Synoptic climatological analyses of extreme snowfalls in the sierra nevada. *Weather and Forecasting* 24, 1610–1624. doi:[10.1175/2009WAF2222249.1](https://doi.org/10.1175/2009WAF2222249.1).

- Pendergrass, A.G., Knutti, R., Lehner, F., Deser, C., Sanderson, B.M., 2017. Precipitation variability increases in a warmer climate. *Scientific Reports* 7, 17966. doi:[10.1038/s41598-017-17966-y](https://doi.org/10.1038/s41598-017-17966-y).
- Pepin, N., Bradley, R.S., Diaz, H.F., Baraer, M., Caceres, E.B., Forsythe, N., Fowler, H., Greenwood, G., Hashmi, M.Z., Liu, X.D., Miller, J.R., Ning, L., Ohmura, A., Palazzi, E., Rangwala, I., Schöner, W., Severskiy, I., Shahgedanova, M., Wang, M.B., Williamson, S.N., Yang, D.Q., Group, M.R.I.E.W., 2015. Elevation-dependent warming in mountain regions of the world. *Nature Climate Change* 5, 424–430. doi:[10.1038/nclimate2563](https://doi.org/10.1038/nclimate2563).
- Poff, N.L., Allan, J.D., Bain, M.B., Karr, J.R., Prestegard, K.L., Richter, B.D., Sparks, R.E., Stromberg, J.C., 1997. The natural flow regime. *BioScience* 47, 769–784.
- Qin, Y., Abatzoglou, J.T., Siebert, S., Huning, L.S., AghaKouchak, A., Mankin, J.S., Hong, C., Tong, D., Davis, S.J., Mueller, N.D., 2020. Agricultural risks from changing snowmelt. *Nature Climate Change* 10, 459–465. doi:[10.1038/s41558-020-0746-8](https://doi.org/10.1038/s41558-020-0746-8).
- Rhoades, A.M., Jones, A.D., Ullrich, P.A., 2018a. Assessing Mountains as Natural Reservoirs With a Multimetric Framework. *Earth's Future* 6, 1221–1241. doi:[10.1002/2017EF000789](https://doi.org/10.1002/2017EF000789).
- Rhoades, A.M., Jones, A.D., Ullrich, P.A., 2018b. The Changing Character of the California Sierra Nevada as a Natural Reservoir. *Geophysical Research Letters* 45, 13,008–13,019. doi:<https://doi.org/10.1029/2018GL080308>.

- Rhoades, A.M., Ullrich, P.A., Zarzycki, C.M., 2018c. Projecting 21st century snowpack trends in western USA mountains using variable-resolution CESM. *Climate Dynamics* 50, 261–288. doi:[10.1007/s00382-017-3606-0](https://doi.org/10.1007/s00382-017-3606-0).
- Scott, D., 2006. *Global Environmental Change and Mountain Tourism*. Routledge, London. chapter 3. p. 54–75. doi:[10.4324/9780203011911](https://doi.org/10.4324/9780203011911).
- Seaber, P., Kapinos, F., Knapp, G., 1987. Hydrologic unit maps. U.S. Geological Survey Water-Supply Paper 2294 , 1–66doi:[https://doi.org/10.1016/S0034-4257\(02\)00098-6](https://doi.org/10.1016/S0034-4257(02)00098-6).
- Serreze, M.C., Clark, M.P., Armstrong, R.L., McGinnis, D.A., Pulwarty, R.S., 1999. Characteristics of the western united states snowpack from snowpack telemetry (snotel) data. *Water Resources Research* 35, 2145–2160. doi:<https://doi.org/10.1029/1999WR900090>.
- Skiles, S., Painter, T.H., 2016. A nine-year record of dust on snow in the colorado river basin, in: Ralston, B. (Ed.), *Proceedings of the 12th Biennial Conference of Research on the Colorado River Plateau*, U.S. Geological Survey Scientific Investigations Report 2015–5180. pp. 1–128. doi:[10.3133/sir20155180](https://doi.org/10.3133/sir20155180).
- Sterle, K., Hatchett, B.J., Singletary, L., Pohll, G., 2019. Hydroclimate Variability in Snow-Fed River Systems: Local Water Managers’ Perspectives on Adapting to the New Normal. *Bulletin of the American Meteorological Society* 100, 1031–1048. doi:[10.1175/BAMS-D-18-0031.1](https://doi.org/10.1175/BAMS-D-18-0031.1).
- Stieglitz, M., Déry, S.J., Romanovsky, V.E., Osterkamp, T.E., 2003. The role

- of snow cover in the warming of arctic permafrost. *Geophysical Research Letters* 30. doi:<https://doi.org/10.1029/2003GL017337>.
- Sturm, M., Goldstein, M.A., Parr, C., 2017. Water and life from snow: A trillion dollar science question. *Water Resources Research* 53, 3534–3544. doi:<https://doi.org/10.1002/2017WR020840>.
- Sumargo, E., Cayan, D.R., 2018. The influence of cloudiness on hydrologic fluctuations in the mountains of the western united states. *Water Resources Research* 54, 8478–8499. doi:<https://doi.org/10.1029/2018WR022687>.
- Svoboda, M., LeComte, D., Hayes, M., Heim, R., Gleason, K., Angel, J., Rippey, B., Tinker, R., Palecki, M., Stooksbury, D., Miskus, D., Stephens, S., 2002. The drought monitor. *Bulletin of the American Meteorological Society* 83, 1181–1190. doi:[10.1175/1520-0477-83.8.1181](https://doi.org/10.1175/1520-0477-83.8.1181).
- Trujillo, E., Molotch, N.P., 2014. Snowpack regimes of the western united states. *Water Resources Research* 50, 5611–5623. doi:<https://doi.org/10.1002/2013WR014753>.
- Ullrich, P.A., Xu, Z., Rhoades, A., Dettinger, M., Mount, J., Jones, A., Vahmani, P., 2018. California’s Drought of the Future: A Midcentury Recreation of the Exceptional Conditions of 2012–2017. *Earth’s Future* 6, 1568–1587. doi:[10.1029/2018EF001007](https://doi.org/10.1029/2018EF001007).
- Viviroli, D., Dürr, H.H., Messerli, B., Meybeck, M., Weingartner, R., 2007. Mountains of the world, water towers for humanity: Typology, mapping, and global significance. *Water Resources Research* 43. doi:<https://doi.org/10.1029/2006WR005653>.

- Wheeler, M.C., Hendon, H.H., 2004. An all-season real-time multivariate mjo index: Development of an index for monitoring and prediction. *Monthly Weather Review* 132, 1917–1932. doi:[10.1175/1520-0493\(2004\)132<1917:AARMMI>2.0.CO;2](https://doi.org/10.1175/1520-0493(2004)132<1917:AARMMI>2.0.CO;2).
- Xu, Y., Jones, A., Rhoades, A., 2019. A quantitative method to decompose SWE differences between regional climate models and reanalysis datasets. *Scientific Reports* 9, 16520. doi:[10.1038/s41598-019-52880-5](https://doi.org/10.1038/s41598-019-52880-5).
- Yan, H., Sun, N., Wigmosta, M., Skaggs, R., Hou, Z., Leung, R., 2018. Next-Generation Intensity-Duration-Frequency Curves for Hydrologic Design in Snow-Dominated Environments. *Water Resources Research* 54, 1093–1108. doi:<https://doi.org/10.1002/2017WR021290>.
- Yarnell, S.M., Stein, E.D., Webb, J.A., Grantham, T., Lusardi, R.A., Zimmerman, J., Peek, R.A., Lane, B.A., Howard, J., Sandoval-Solis, S., 2020. A functional flows approach to selecting ecologically relevant flow metrics for environmental flow applications. *River Research and Applications* 36, 318–324. doi:<https://doi.org/10.1002/rra.3575>.
- Zeng, X., Broxton, P., Dawson, N., 2018. Snowpack change from 1982 to 2016 over conterminous united states. *Geophysical Research Letters* 45, 12,940–12,947. doi:[10.1029/2018GL079621](https://doi.org/10.1029/2018GL079621).

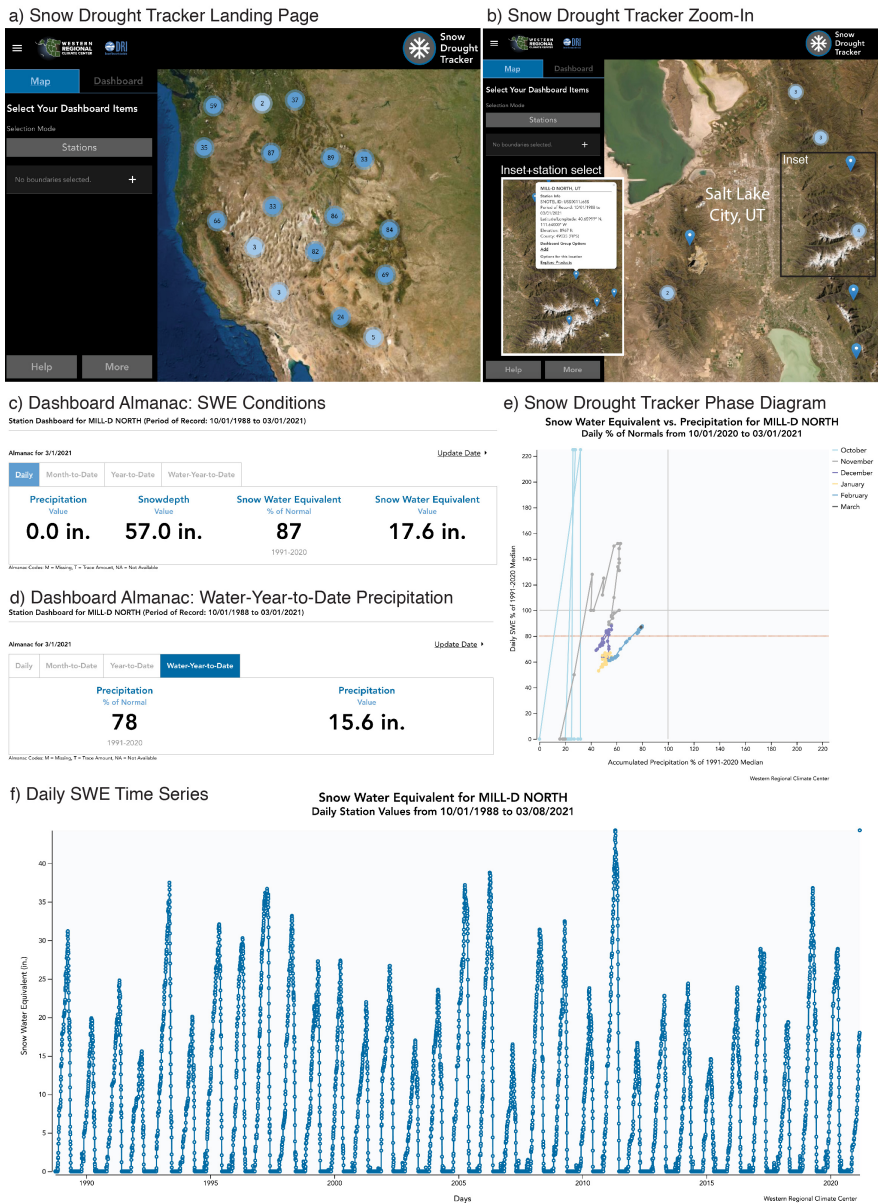


Figure 8: Screenshots from the beta Western Regional Climate Center (WRCC)'s Snow Drought Tracker. (A) Snow Drought Tracker Dashboard landing page. (B) Example of zooming in to region and a station with station information upon selection (inset). (C-D) Almanac tabs. (E) Real-time phase diagram for water year 2021. (F) Daily snow water equivalent (SWE) time series for the period of record.